Elastic properties in quantum ferroelectric $KTa_{1-x}Nb_xO_3$

D. Rytz and A. Châtelain
Institute of Experimental Physics, Swiss Federal Institute of Technology, CH-1015, Lausanne, Switzerland

U. T. Höchli*
Istituto di Fisica dell'Università degli Studi di Pavia, I-27100 Pavia, Italy

(Received 22 February 1983)

Elastic compliance measurements are reported in $KTa_{1-x}Nb_xO_3$ mixed crystals exhibiting a concentration-dependent ferroelectric phase-transition temperature T_c. For concentrations $x \geq 0.008$, an anomaly is observed at T_c in the temperature dependence of the elastic compliance s_{11}, consisting of a steplike discontinuity with a superimposed Curie-Weiss-type singularity. The critical exponent μ, defined by $s_{11} \sim (T-T_c)^{-\mu}$, varies from $\mu=1.3$ for $x=0.05$ to $\mu=1.9$ for $x=0.008$. As x is lowered towards 0.008, the amplitude of the step discontinuity is largely unaffected. For $x<0.008$, no anomaly occurs. The experimental results are compared to dielectric data sets previously obtained, and interpreted in the light of renormalization-group predictions. A specific quantum critical behavior is obtained for transition temperatures $T_c<30$ K.

I. INTRODUCTION

$KTa_{1-x}Nb_xO_3$ is a well-known mixed-crystal series whose ferroelectric transition temperature varies linearly with Nb concentration x as[1,2]

$$T_c = 676x + 32 , \quad (1)$$

measured in K. This law is valid in the concentration range $0.05 \leq x \leq 1.00$, where T_c increases from 65 K in $KTa_{0.05}Nb_{0.95}O_3$ to 708 K in pure $KNbO_3$. The low concentration range $x<0.05$ has attracted much interest in recent times. The transition temperature was found to depend on concentration as[3]

$$T_c = 276(x-0.008)^{1/2} , \quad (2)$$

measured in K. This quadratic T_c vs x function appeared to be typical of quantum ferroelectrics. The fact that beyond a critical concentration $x_c=0.008$ no ferroelectric phase transition is observed agrees with the established stability of the paraelectric phase in pure $KTaO_3$ down to the lowest temperature $T=1.5$ K at which dielectric measurements are performed.[4] In addition to the early measurements of the dielectric constant and the elastic compliance,[3,5] Raman scattering studies[5] have been performed: All the data sets are consistent with Eq. (2).

After initial attempts to elucidate the nature of the dielectric anomaly in $KTa_{1-x}Nb_xO_3$,[7,8] it appeared desirable to investigate the corresponding elastic anomaly. This is the purpose of this paper, which presents a study of the critical behavior exhibited by the elastic compliance as a function of concentration x and temperature T. This study should serve to deepen the understanding of quantum ferroelectricity in the light of recent ultrasonic studies near phase transitions.[9,10]

The outline of this paper is as follows. In Sec. II, we review sample preparation and experimental technique before displaying the experimental results. We also analyze the effect of the inhomogeneous Nb concentration in detail. Section III discusses the properties of quantum ferroelectrics in the framework of recent theories on the critical phenomena. Conclusions are summarized in Sec. IV.

II. EXPERIMENT

A. Crystal growth and sample preparation

The $KTa_{1-x}Nb_xO_3$ crystals were grown from the melt by a slow-cooling method. The growth experiments are described in some detail in Ref. 11. An especially adapted stirring method known as the accelerated crucible rotation technique[12] was successfully employed to achieve nucleation control, increase the growth rate, and, most importantly, to minimize inhomogeneity. A typical growth run is schematically shown in Fig. 1. The starting oxides and carbonates are brought to reaction in a sealed platinum crucible at high temperature to form the starting melt of Nb concentration x_m:

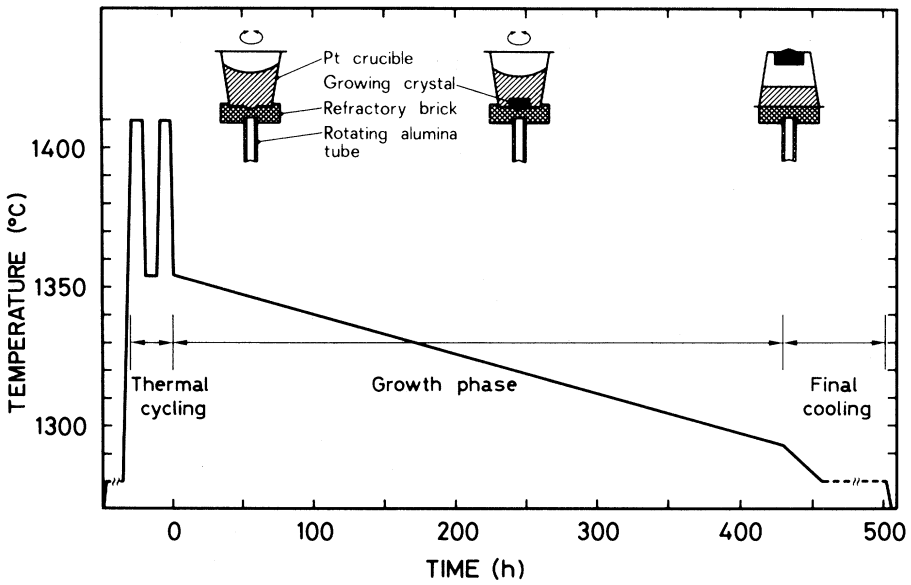

FIG. 1. Temperature vs time curve for growth experiment KB 30 resulting in one $26\times24\times16$ mm^3 $KTa_{1-x}Nb_xO_3$ crystal. Also shown is the position of the crucible during the three steps of the run.

$$(1-x_m)Ta_2O_5+x_mNb_2O_5+K_2CO_3 \rightarrow 2KTa_{1-x_m}Nb_{x_m}O_3+CO_2\,. \quad (3)$$

An excess of K_2CO_3 is always maintained in order for it to act as a flux. After a period of thermal cycling, the cooling program sets in at a starting temperature T_0. The actual temperature T_1 where growth starts is unknown. The experiment is terminated by inverting the crucible at a temperature T_2 which is empirically determined. The crystal is then free of the remaining melt, and may subsequently be cooled down to room temperature. The parameters pertinent to one of the crystals used in the following study are listed in Table I.

The Nb concentration x in the crystal was determined in an electron microprobe experiment.[10] It is lower than x_m, in agreement with the $KTaO_3$-$KNbO_3$ phase diagram.[13,14] It was also shown that $KTa_{1-x}Nb_xO_3$ mixed crystals exhibit a concentration gradient along the $\langle 100\rangle$ direction with, possibly, superimposed striations. These striations are minimized by the use of the accelerated crucible rotation technique. The remaining gradient is inherent to a cooling experiment. A typical value is

$$(\Delta x/\Delta z)_{\langle 100\rangle}\approx 0.0005, \quad (4)$$

measured in mol/mm. The gradient will show up along the growth direction z, parallel to $\langle 100\rangle$. Therefore optimum cuts should result in probes with their smallest dimension along z.

The probes required for our experiments were parallelepipedic-shaped bars of approximately $8\times1\times0.6$ mm^3. With few exceptions, the edges were cut along $\langle 100\rangle$ directions. The surfaces were optically polished with diamond paste (6 and 2 μm) on a Teflon cylinder. The major faces were coated with a double-layered chromium plus gold electrode. The probes were then bonded with a silver-paint dot to two 25-μm-diam gold wires and mounted in a suitable sample holder enabling operation from 1.4 to 400 K.

Table II gives an overview of the properties of various probes, in particular, their concentration; the corresponding transition temperatures and elastic softenings are to be discussed later. Here we shall explicate the five different categories of probes used in the present investigation. The symbols KA, KB, and KC refer to our own growth experiments: KA were preliminary runs based on a simple cooling

TABLE I. Parameters of a $KTa_{1-x}Nb_xO_3$ growth experiment.

Experiment	x_m	Duration	T_0(°C)	T_2(°C)	Crystal (weight, size)	x
KB 30	0.030	430 h	1354	1293	83 g, ($26\times24\times16$ mm^3)	0.008 ± 0.002

TABLE II. Composition x, transition temperature T_c, and relative softening $\Delta(s_{11}^{-1})/(s_{11}^{-1})$ at 4.2 K for various $KTa_{1-x}Nb_xO_3$ samples. An asterisk designates the probes analyzed with the aid of an electron microprobe. ACRT stands for accelerated crucible rotation technique.

Sample		x (mol)	T_c (K)	$\Delta(s_{11}^{-1})/(s_{11}^{-1})$
KA KT 0		0		0
MIT MIT	grown at MIT	0		0
KA KT 2		0.003		0
KC PK 1		0.006		0.06
KB KSK 30 |I|	grown with ACRT	0.0075*		0.21
KB KSK 30 |III|	grown with ACRT	0.008	5.0	0.27
KB KSK 30 |IV|	grown with ACRT	0.009*	8.0	0.36
KB KSK 45	grown with ACRT	0.009*	8.4	0.36
KB KSK 30 |*A*|	grown with ACRT	0.009	8.5	0.37
KB KSK 30 |*B*|	grown with ACRT	0.009	8.9	0.38
KB KSK 30 |*L*|	grown with ACRT	0.009	9.1	0.39
KB KSK 30 |VI|	grown with ACRT	0.009*	9.3	0.36
KB KSK 30 |VII|	grown with ACRT	0.009*	10.0	0.43
KB KSK 51	grown with ACRT	0.012	17.6	0.48
KA KT 4		0.019	29.0	0.52
KB KSK 10 |4|	grown with ACRT	0.021	32.2	0.56
KB KSK 4		0.029	41.0	0.58
KA KT 8		0.057	66.6	0.58
AER AER 44	grown at Aerospace	0.15	131.2	
AER AER 40	grown at Aerospace	0.18	152.3	
KC PK 9		0.20	170.3	
KC PK 3		0.29	226.4	
KC PK 8		0.36	273.8	

method developed for pure $KTaO_3$,[15] and KB designates the slow-cooling experiments previously discussed. Both were aimed at the production of crystals in the low concentration range $0 \leq x < 0.06$. The KB method has recently been extended to a much broader concentration range $0 < x \leq 0.45$ in the KC experiments.[16] We shall comment on the differences between samples from various origins in the next section, and also take into account our measurements on crystals grown elsewhere; a $KTaO_3$ grown at Massachusetts Institute of technology (designated in Table II by MIT) by the top-seeded-solution method,[17] and two $KTa_{1-x}Nb_xO_3$ grown at Aerospace Corporation (designated in Table II by AER) by a slow-cooling method.[18]

B. Elastic behavior in $KTa_{1-x}Nb_xO_3$

1. *The acoustic-resonance technique*

In an acoustic experiment, a length-extensional vibration is excited by a transverse ac field. Basically, the sample with its parallelepipedic shape is a parallel-plate capacitor. Because of piezoelectric coupling, when the frequency of the alternating electric field corresponds to the mechanical resonance frequency f of the sample, a maximum is observed in the conductance, whereas the capacitance shows dispersive behavior. A detailed discussion on the determination of electromechanical parameters may be found elsewhere.[19–22] For a bar of length l and density ρ, the resonance frequency yields a direct measurement of the inverse elastic compliance s_{11}^{-1}:

$$s_{11}^{-1} = 4\rho l^2 f^2 , \tag{5}$$

provided the length l exceeds the width and the thickness of the bar by an order of magnitude. It is essential that the thickness is not below ~ 250 μm in order to avoid frequency shifts due to surface layers.[23]

For the evaluation of the data, the temperature dependence of ρ and l was neglected. Given the thermal-expansion coefficient 5×10^{-6} K^{-1} as obtained for $KTaO_3$ in Refs. 24 and 25, the variation of s_{11}^{-1} due to $\partial\rho/\partial T$ and $\partial l/\partial T$ is 2 orders of magnitude smaller than that of $\partial f/\partial T$ observed direct.

Piezoelectricity was induced by applying a dc electric field.[21] Owing to the large polarizability of the material, moderate fields of ~ 0.2 MV/m are sufficient to observe acoustic resonance. The frequency shift induced was determined by extrapolation to zero field and seen to be negligible for the fields applied in the experiments.

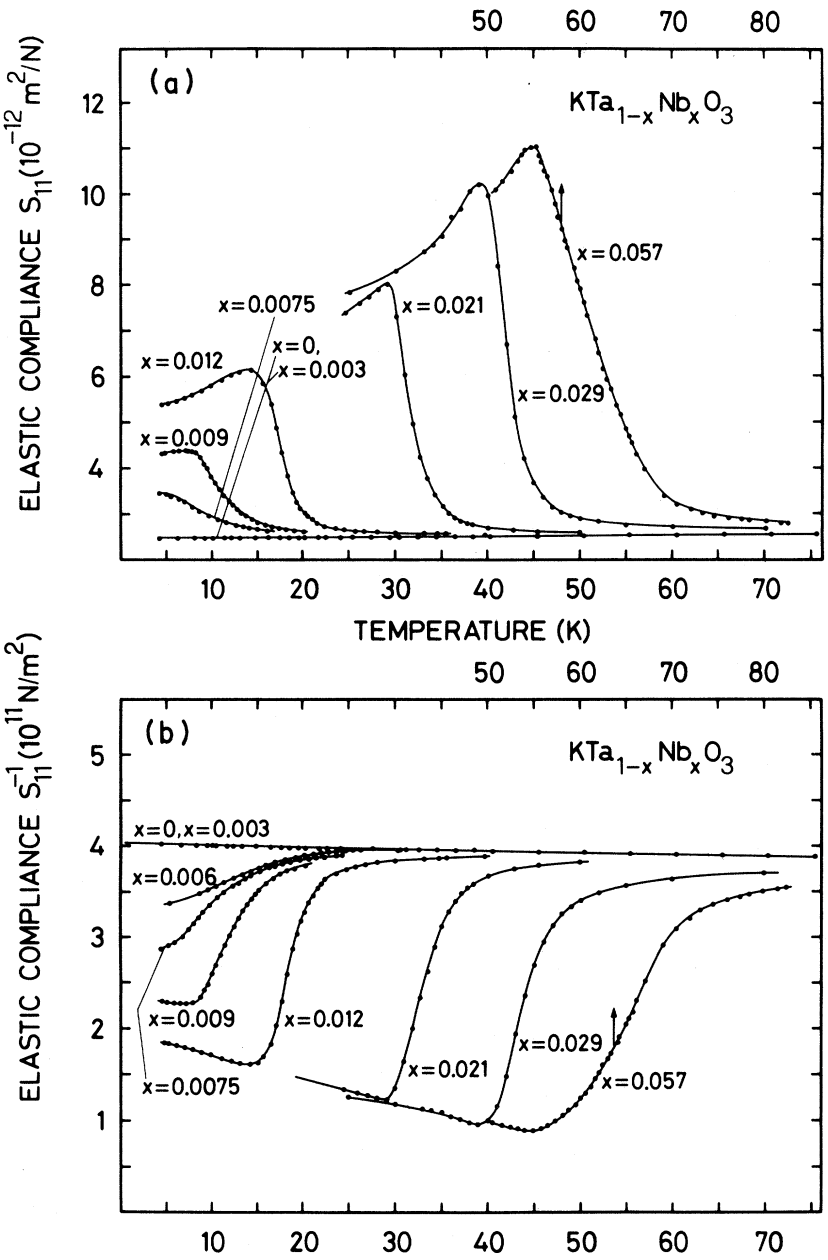

FIG. 2. Temperature dependence of the elastic compliance s_{11} (a) and of its inverse (b) with concentration x as a parameter. The data were obtained under a bias field $E_{dc} \approx 10$ kV/m applied after cooling. The temperature was changed at a rate of no more than 0.5 K/min. Note the change on the temperature scale for $x=0.057$.

2. *Acoustic-resonance results*

Our main effort here is aimed at separating two contributions to the elastic anomaly at T_c in $KTa_{1-x}Nb_xO_3$, and at analyzing their concentration dependence. By extending thereby elastic data previously reported[3] to a wider concentration range ($0 \leq x \leq 0.36$), it will be possible to separate different regimes, and to observe the distinguishing features of the elastic behavior of quantum ferroelectrics.

The fairly large amount of data is organized as follows: Figure 2(a) shows the elastic compliance s_{11} as a function of temperature T for several low Nb concentrations ($0 \leq x < 0.06$). At T_c, a marked critical anomaly of the Curie-Weiss type $\Delta s = A(T - T_c)^{-\mu}$ is clearly evidenced. Figure 2(b) displays the inverse elastic compliance s_{11}^{-1} for the same set of concentrations. In this picture, the

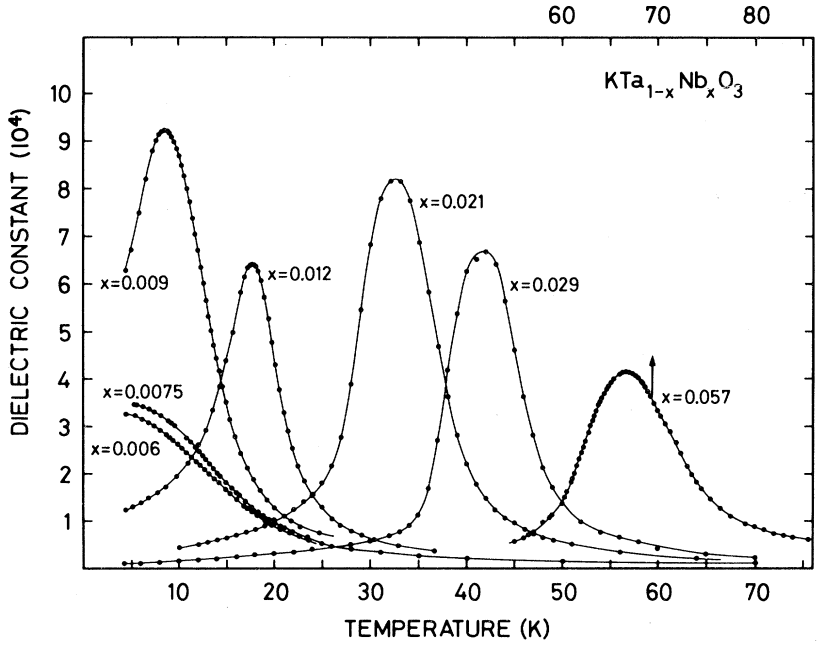

FIG. 3. Temperature dependence of the static dielectric constant ϵ with concentration x as a parameter. The data were obtained by a conventional bridge technique at 1 kHz. The temperature was changed at a rate of no more than 0.5 K/min. Note the change on the temperature scale for $x=0.057$.

Curie-Weiss anomaly appears to be quenched and the experimental curves suggest a strong steplike discontinuity (with finite width). Close to T_c, the $s_{11}(T)$ function is a superposition of the step plus the Curie-Weiss singularity. This second contribution to the elastic anomaly has not been sufficiently well resolved in previous studies.[3] Figure 3 shows the Curie-Weiss behavior found for the dielectric constant, and establishes the close correspondence of the respective T_c's for the dielectric and elastic peaks. Before we analyze these data, we plot in Fig. 4 $s_{11}(T)$ and $s_{11}^{-1}(T)$ for $KTa_{1-x}Nb_xO_3$ mixed crystals with larger concentrations ($0.18 \leq x \leq 0.36$) and, for the sake of comparison, also for $SrTiO_3$.[26]

Common to all curves is the temperature coefficient far above T_c: In terms of the effective elastic rigidity, we observe, for $T-T_c > 20$ K and for all x's, a relative variation equal to

$$[s_{11}^{-1}(T)-s_{11}^{-1}(o)]/[s_{11}^{-1}(0)T] \approx 3.3\times 10^{-4}\ , \tag{6}$$

measured in K^{-1}. Below T_c, some acoustic loss is encountered in all the samples. It is attributed to the motion of domain walls under the influence of the driving field (a phenomenon known as "ΔE effect," see Ref. 27 for an analysis in $SrTiO_3$). Therefore no evaluation of the data is attempted for $T_c-10<T<T_c$.

For $x<0.0075$, both the dielectric and the elastic peaks are truncated: No transition occurs to the ferroelectric phase at positive temperatures. This suggests a common origin for the leveling off of the dielectric constant and of the elastic compliance. The quantum-mechanical stabilization of the paraelectric phase analyzed previously[7] for the dielectric properties is thus also observed in elasticity, as will be discussed in Sec. III. For $x \geq 0.0075$, the elastic anomalies in $KTa_{1-x}Nb_xO_3$ and in $SrTiO_3$ look much alike, except for a broadening of the response in $KTa_{1-x}Nb_xO_3$. It is tempting to attribute this broadening to compositional inhomogeneities. Improved control of crystal growth allows us to check experimentally the role of inhomogeneity in the elastic compliance measurements.

To test the influence of concentration gradients, three probes were measured, all cut from one single crystal. One of them (L) had its length parallel to the growth direction z, the other two (A,B) were perpendicular to z [see Fig 5(a)]. Following the remarks developed in the preceeding section, L is less homogeneous than A or B because its length is parallel to the concentration gradient. Figure 5(b) displays the changes in the inverse elastic compliance due to the increase of the Nb concentration as a function of position in the as-grown sample. The concentration values that could be deduced from the phase diagram when measuring the T_c's (see Refs. 3, 7, and also Sec. III) via the dielectric peak are in agreement with the electron microprobe value

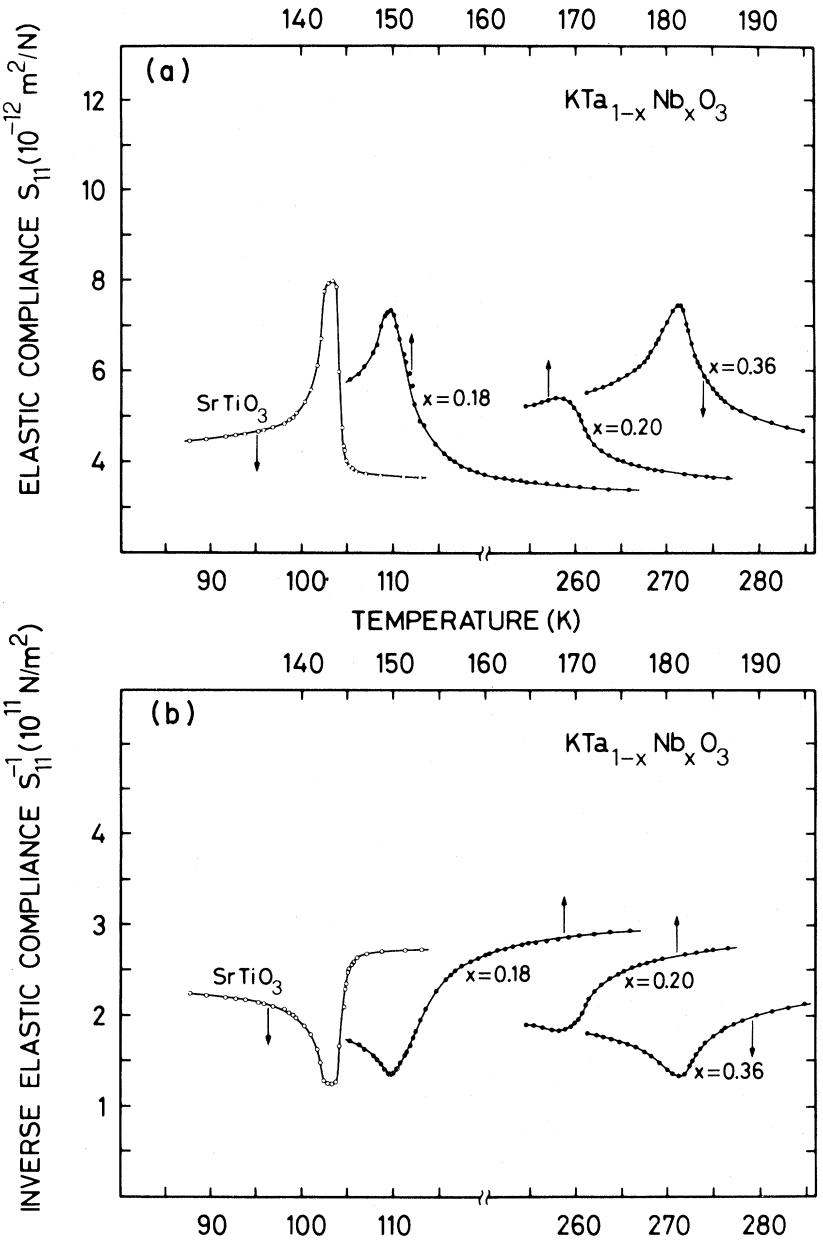

FIG. 4. Temperature dependence of the elastic compliance s_{11} (a) and of its inverse (b) with concentration x as a parameter. The functions $s_{11}(T)$ and $s_{11}^{-1}(T)$ of a $SrTiO_3$ crystal are also shown for comparison.

$x=0.008\pm0.002$. In this small concentration range, the resolution of such a microprobe experiment is insufficient to visualize the small differences from sample to sample. The concentration gradient, however, is well established. Inspection of Fig. 5(a) shows that the mean concentration of L is larger than that of A or B, the elastic step of L being also more important. The shape of the curve does not appear to be strongly modified by inhomogeneity except for a slightly more pronounced rounding of the anomaly near T_c. This effect is evidenced in Fig. 5(c) where the inhomogeneous probe, cut along a $\langle 111 \rangle$ direction (therefore having a nonzero projection on the concentration gradient), gives rise to an elastic step without any anomaly. In this geometry, the elastic compliance would be $2s_{11}+2s_{12}+s_{44}-4s_{12}^2/s_{11}$, and thus an anomaly in s_{11} should be detectable. The influence of inhomogeneity can also be seen in Fig. 2, when closely inspecting the probe with $x=0.057$. There the curve is markedly

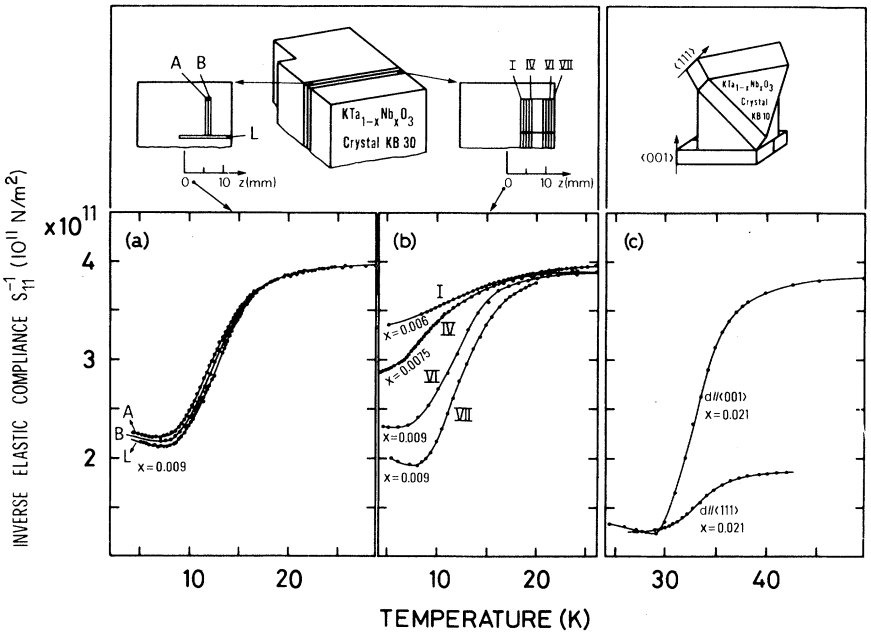

FIG. 5. Temperature dependence of the inverse elastic compliance for various probes precisely located with respect to the concentration gradient in the as-grown crystal. (a) shows the effect observed for probes parallel and perpendicular to the gradient directed along the growth direction z. (b) describes the gradient itself. (c) indicates the effect for different orientations. It should be noted that the inverse elastic compliance is $2s_{11}+2s_{12}+s_{44}-4(s_{12}^2/s_{11})$ when the thickness of the sample is along ⟨111⟩.

rounded near T_c. For this probe, inhomogeneity is especially large when compared to the other crystals (which were grown with the KB method). This was due, precisely, to the growth method KA leading inherently to large concentration gradients.

We conclude that the primary effect of inhomogeneity is to round off the Curie-Weiss anomaly at T_c. The width of the elastic step and the steepness of the inverse elastic compliance versus temperature seem to remain unaffected. Thus in the present samples, the effects observed reflect intrinsic properties of the $KTa_{1-x}Nb_xO_3$ crystals, the distribution of T_c's playing a minor role.[28]

III. INTERPRETATION

It appears worthwhile analyzing first the results extrapolated at zero temperature for various concentrations, and second the data at given concentrations as a function of temperature. The first step permits us to test the results of a renormalization-group prediction taking into account quantum effects for phase transitions near the quantum limit. The second step allows us to interpret the two superimposed anomalies in $s_{11}(T)$.

Let us begin by recalling some results of recent renormalization-group work[29,30] dealing with phase transitions in the quantum regime. At zero temperature the following laws are predicted for the transition temperature T_c, the order parameter P, and the zero-point dielectric susceptibility ϵ^{-1}:

$$T_c \sim (x - x_c)^{1/2} , \tag{7}$$

$$P(T=0) \sim (x - x_c)^{1/2} , \tag{8}$$

$$\epsilon^{-1}(T=0) \sim (x - x_c) , \tag{9}$$

where x is called "interaction parameter" and may have a more general sense than the mere Nb concentration in $KTa_{1-x}Nb_xO_3$. Our data displayed in Figs. 6(a) and 6(b) support Eqs. (7) and (9), respectively, and extend previous measurements[3,7] of the same quantities. It should be noted that the resulting critical exponents (in x space) assume the values predicted by mean-field theory.[31] Mean-field theory applied to the case of cubic perovskites[32] predicts a steplike discontinuity for the elastic compliance. The measurements leading to Fig. 6(c) confirm this theoretical prediction in x space: At $x = x_c$, an elastic step is observed experimentally. From these considerations, we concluded that *mean-field behavior* provides a correct description in interaction-parameter space of quantum ferroelectrics.

An analysis of the temperature dependence of the elastic compliance in $KTa_{1-x}Nb_xO_3$ for a given

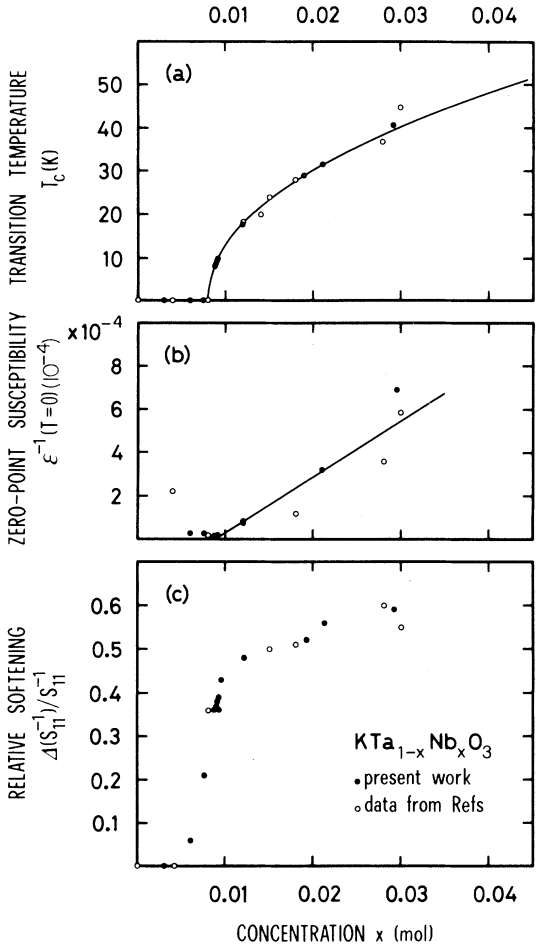

FIG. 6. Transition temperature (a), zero-point susceptibility (b), and elastic softening (c) vs x in $KTa_{1-x}Nb_xO_3$ mixed crystals. Data from previous work are also reported. In Ref. 11 the concentration was calibrated in an electron microprobe experiment. In the present work, a few values of x were again checked with the same type of experiment (see Table I), the other concentrations being deduced from the corresponding transition temperatures. The elastic softening is defined as

$$\frac{\Delta(s_{11}^{-1})}{s_{11}^{-1}}=\frac{s_{11}^{-1}(300\text{ K})-s_{11}^{-1}(0)}{s_{11}^{-1}(300\text{ K})}\ .$$

concentration x can be made in analogy with $SrTiO_3$. For the structural phase transition occurring at $T_c=105$ K in $SrTiO_3$, the elastic step (in T space) predicted by theory[32] was verified experimentally,[9,21] except in the immediate vicinity of T_c. The data near T_c were recently explained[10] in terms of critical fluctuations. When merely intrinsic fluctuations of the order parameter were concerned, it was found that, for $T>T_c$,

$$\Delta s_{11}=s_{11}(T)-s_{11}(\infty)\sim(T-T_c)^{-0.4}. \tag{10}$$

However, if fluctuations are driven by mobile impurities, then

$$\Delta s_{11}\sim(T-T_c)^{-2(\gamma-2\beta)}\ , \tag{11}$$

where γ and β are the usual critical exponents for susceptibility and order parameter, respectively. For Heisenberg-type critical behavior, for example, $2(\gamma-2\beta)$ is approximately equal to 1.3.[10] Thus we analyze our elastic compliance data in terms of

$$s_{11}=s_{11}^0+A(T-T_c)^{-\mu}\ , \tag{12}$$

where A and μ are constants: s_{11}^0 has the form $B+CT$, and acts as a background that can be obtained from data taken far from T_c. For $SrTiO_3$, the experiment[10] assigns $\mu=1.5\pm0.2$. For $KTa_{1-x}Nb_xO_3$, we report $s_{11}-s_{11}^0$ as a function of $T-T_c$ in a doubly logarithmic plot (see Fig. 7), and obtain values of μ varying from 1.3 to 1.9. From earlier investigations of the dielectric susceptibility,[7] we know that the exponent γ reaches the value 2.0 at the ferroelectric quantum limit, and decreases down to the classical value $\gamma=1$ with increasing concentration. Although β is not known very accurately, it is expected from spontaneous polarization measurements[33] that it remains approximately equal to 0.5 for all the x concentrations investigated here. Thus the variation of β with x remains small compared to the important change of γ: Therefore a decrease of μ with increasing x is expected. Qualitatively, this prediction is verified in $KTa_{1-x}Nb_xO_3$ (see Fig. 7). However, the seemingly good fits are far from allowing a quantitative determination. In part, this may be due to the uncertainty in T_c as evidenced by the relative displacement between the peaks of s_{11} and ϵ, and in part due to inhomogeneous broadening of the responses.

These results may be summarized as follows: In $SrTiO_3$ near its 105 K transition as well as in $KTa_{1-x}Nb_xO_3$ with $x\geq0.0075$, the observed critical singularity of the elastic compliance is stronger than that predicted by a theory of ideal-crystal critical behavior, where intrinsic fluctuations would drive the transition. This is indicative of a defect-induced transition mechanism. For the moment, however, the nature and behavior of the impurities involved remain hypothetical.

At transition temperatures below ~10 K (for $x<0.0075$), the analysis in terms of Eq. (12) is no longer significant. In this range, we are left with a mere (broad) step. As shown in Fig. 8, the "amplitude" (related to the Curie constant) of the critical Curie-Weiss-type anomaly decreases with decreasing x. In fact, it scales as T_c:

$$[s_{11}^{\max}-s_{11}(0)]/s_{11}(0)\sim T_c\ . \tag{13}$$

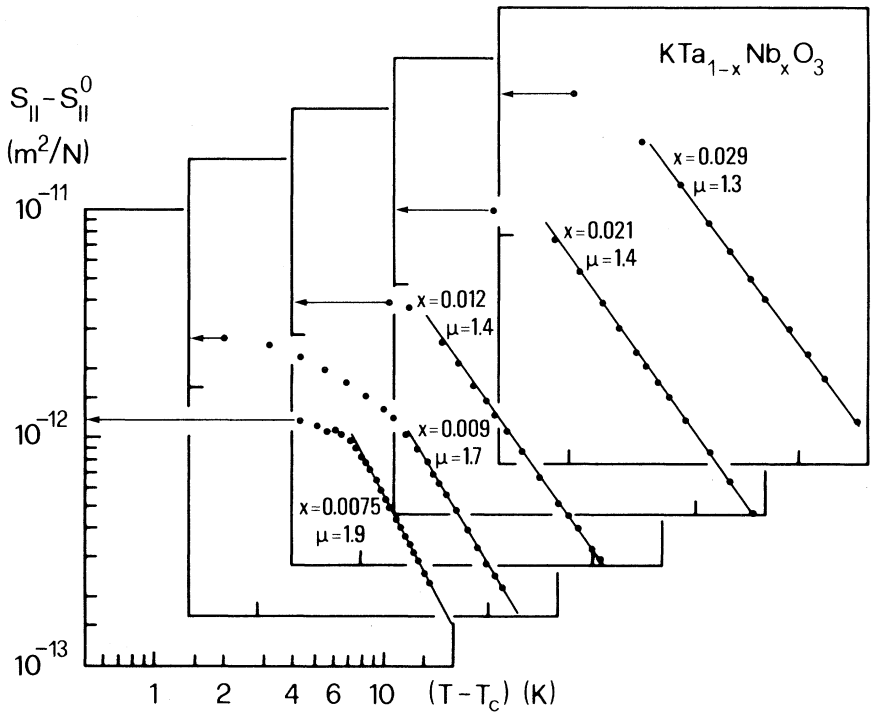

FIG. 7. Doubly logarithmic plots of $s_{11}-s_{11}^0$ vs $T-T_c$ for various Nb concentrations x. The steepness of the curve determines the critical exponent μ. T_c was taken as the temperature where the peak of the dielectric constant takes place. By choosing T_c as the temperature corresponding to the maximum of s_{11}, the exponent μ would shift to lower values (by 0.1—0.2) and lead to fits of inferior quality.

This is reminiscent of the vanishing of the Curie-Weiss anomaly for the dielectric constant. From numerous measurements in quantum-ferroelectric $KTa_{1-x}Nb_xO_3$ (Refs. 3 and 7) and paraelectric $KTaO_3$ (Ref. 4) and $SrTiO_3$,[34] is is known that the dielectric constant levels off at low temperatures (see also Fig. 3: For $x=0.006$, a stabilization occurs below ~ 6 K). This is attributed to the quantum-mechanical stabilization of the paraelectric phase. In analogy with ϵ, s_{11} is also stabilized at low temperatures and the Curie-Weiss anomaly vanishes. As a consequence, we have to admit that the hypothetical mobile impurity freezes out upon cooling, before the quantum T_c is reached. This freezing phenomenon differentiates the classical from the quantum regimes.

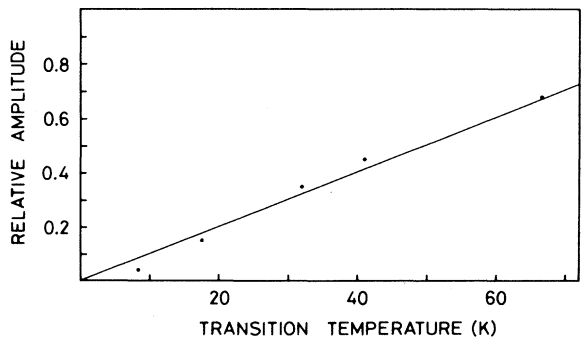

FIG. 8. Relative amplitude $[s_{11}^{max}-s_{11}(0)]/s_{11}(0)$ vs T_c, where s_{11}^{max} is the peak value of the anomaly in s_{11}.

Before summarizing our results, we should like to mention two extensions of the present work that appear worth exploring further. Firstly, the nature of this hypothetical impurity that drives the transitions should be investigated. An experimental approach for such an identification could consist of measuring the dispersion phenomena associated with the freezing out, possibly with the help of a magnetic-resonance (EPR or NMR) technique. Secondly, the latest developments of a very recent theory on quantum critical phenomena[35–37] provide an improved description of the role played by zero-point fluctuations. In the framework of this stochastic quantization approach, new results are to be expected that may lead to a deeper understanding of quantum-ferroelectric phase transitions.

IV. SUMMARY

Our measurements of the elastic properties of $KTa_{1-x}Nb_xO_3$ mixed crystals may be summarized as follows:

(i) As a function of concentration x, a steplike discontinuity at a critical concentration x_c is obtained in the behavior of the inverse elastic compliance s_{11}^{-1}. The critical concentration is $x_c=0.008$, above which $KTa_{1-x}Nb_xO_3$ is ferroelectric at zero temperature.

(ii) As a function of temperature and for a fixed concentration $x \geq 0.008$, a steplike anomaly is observed for s_{11}^{-1} with a critical Curie-Weiss singularity superimposed.

(iii) The size of the elastic step varies little with x (or with T_c), provided there is a phase transition, whereas the Curie-Weiss singularity is governed by a Curie constant proportional to T_c.

Several conclusions may be drawn from the experiments:

(iv) The observation of a step in s_{11}^{-1} as a function of x, i.e., mean-field behavior in x space, verifies the prediction of a renormalization-group calculation valid for phase transitions in the quantum regime ($x \approx x_c$), where zero-point fluctuations are important.

(v) For $x \geq x_c$, a Curie-Weiss law $s_{11} \sim (T-T_c)^{-\mu}$, with μ varying from 1.3 for $x=0.05$ to 1.9 for $x=0.008$, is observed and supports the idea of a defect-induced transition mechanism, the nature of the defect remaining hypothetical, however.

(vi) The disappearance of the Curie-Weiss singularity at $T_c=0$ has the same origin as the previously investigated leveling off of the dielectric anomaly in quantum ferroelectrics. Both the elastic and the dielectric anomalies are indicative for quantum critical phenomena clearly different from their classical counterparts.

ACKNOWLEDGMENT

We are grateful to V. Belruss (MIT) and J. A. Osmer (Aerospace Corp.) for kindly providing some excellent samples used in this study. A preliminary report of this work was communicated at the Swiss Physical Society meeting in Berne (April 1–2, 1982) and an extended abstract has already appeared: D. Rytz and U. T. Höchli, Helv. Phys. Acta 55, 170 (1982).

---

*Permanent address: IBM Zurich Research Laboratory, CH-8803 Rüschlikon, Switzerland.

[1]S. Triebwasser, Phys. Rev. 114, 63 (1959)

[2]C. H. Perry, R. R. Hayes, and N. E. Tornberg, in *Molecular Spectroscopy of Dense Phases,* edited by M. Goossman, S. G. Elkomoss, and J. Ringeisen (Elsevier, Amsterdam, 1976), p. 267.

[3]U. T. Höchli, H. E. Weibel, and L. A. Boatner, Phys. Rev. Lett. 39, 1158 (1977).

[4]S. H. Wemple, Phys. Rev. 137, A1575 (1965).

[5]U. T. Höchli and L. A. Boatner, Phys. Rev. B 20, 266 (1979).

[6]R. L. Prater, L. L. Chase and L. A. Boatner, Phys. Rev. B 23, 221 (1981).

[7]D. Rytz, U. T. Höchli, and H. Bilz, Phys. Rev. B 22, 359 (1980).

[8]R. Kind and K. A. Müller, Commun. Phys. 1, 223 (1976).

[9]B. Lüthi and W. Rehwald, in *Structural Phase Transitions I,* edited by K. A. Müller and H. Thomas (Springer, Berlin, 1981), p. 131.

[10]U. T. Höchli and A. D. Bruce, J. Phys. C 13, 1963 (1980).

[11]D. Rytz and H. J. Scheel, J. Cryst. Growth 59, 468 (1982).

[12]D. Elwell and H. J. Scheel, *Crystal Growth from High-Temperature Solutions* (Academic, London, 1975).

[13]A. Reisman, S. Treibwasser, and F. Holtzberg, J. Am. Chem. Soc. 77, 4228 (1955).

[14]P. D. Garn and S. S. Flaschen, Anal. Chem. 29, 275 (1957).

[15]D. M. Hannon, Phys. Rev. 164, 366 (1967).

[16]D. Rytz (unpublished).

[17]V. Belruss, J. Kalnajs, A. Linz, and R. C. Folweiler, Mater. Res. Bull. 6, 899 (1971).

[18]J. A. Osmer and A. B. Chase (unpublished).

[19]W. P. Mason, *Piezoelectric Crystals and Their Application to Ultrasonics* (Van Nostrand, New York, 1950).

[20]E. Hafuer, Proc. IEEE 57, 179 (1969).

[21]G. Rupprecht and W. H. Winter, Phys. Rev. 155, 1019 (1967).

[22]U. T. Höchli, J. Phys. C 8, 3896 (1975).

[23]J. P. Ansermet, D. Rytz, A Châtelain, U. T. Höchli, and H. E. Weibel, J. Phys. C 14, 4541 (1981).

[24]D. G. Demurov and Yu. N. Venevtsev, Fiz. Tverd. Tela (Leningrad) 13, 696 (1971) [Sov. Phys.—Solid State 13, 553 (1971)].

[25]G. A. Samara and B. Morosin, Phys. Rev. B 8, 1256 (1973).

[26]The $SrTiO_3$ employed here was a top-seeded solution-grown (TSSG) crystal analogous to the TSSG probe used in Ref. 10.

[27]U. T. Höchli, Solid State Commun. 13, 1369 (1973).

[28]See Ref. 3 where inhomogeneity of early samples was believed to cause broadening of the full step.

[29]T. Schneider, H. Beck, and E. Stoll, Phys. Rev. B 13, 1123 (1976).

[30]R. Oppermann and H. Thomas, Z. Phys. B 22, 387

(1975).

[31]H. E. Stanley, *Introduction to Phase Transitions and Critical Phenomena* (Oxford University Press, Oxford, England, 1971).

[32]J. C. Slonczewski and H. Thomas, Phys. Rev. B 1, 3599 (1970).

[33]L. A. Boatner, U. T. Höchli, and H. E. Weibel, Helv. Phys. Acta. 50, 620 (1977).

[34]K. A. Müller and H. Burkard, Phys. Rev. B 19, 3593 (1979); in this work, attention is drawn to the quantum-paraelectric behavior of $SrTiO_3$ and not to its structural transition at 105 K.

[35]M. Zanetti, Phys. Rev. B 22, 5267 (1980).

[36]P. Ruggiero and M. Zanetti, Phys. Rev. Lett. 47, 1231 (1981).

[37]P. Ruggiero and M. Zanetti (unpublished).